Journal of Pharmaceutical and Biomedical Analysis 175 (2019) 112783

Contents lists available at ScienceDirect

Journal of Pharmaceutical and Biomedical Analysis

journal homepage: www.elsevier.com/locate/jpba

Online comprehensive hydrophilic interaction chromatography × reversed phase liquid chromatography coupled to mass spectrometry for in depth peptidomic profile of microalgae gastro-intestinal digests

Eduardo Sommella[a,1], Emanuela Salviati[b,c,1], Fabrizio Merciai[b,c], Michele Manfra[e], Alessia Bertamino[b], Francesco Gasparrini[d], Ettore Novellino[a], Pietro Campiglia[b,f,*]

[a] Department of Pharmacy, University of Naples Federico II, Napoli, Italy
[b] Department of Pharmacy, University of Salerno, Fisciano, SA, Italy
[c] PhD Program in Drug Discovery and Development, University of Salerno, Fisciano, SA, Italy
[d] Dipartimento di Chimica e Tecnologie del Farmaco, Sapienza Università di Roma, P.le Aldo Moro 5, 00185 Roma, Italy
[e] Department of Science, University of Basilicata, Viale dell'Ateneo Lucano 10, I-85100, Potenza, Italy
[f] European Biomedical Research Institute of Salerno (Ebris), Via De Renzi 3, 84125, Salerno, Italy

ARTICLE INFO

Article history:
Received 11 June 2019
Received in revised form 11 July 2019
Accepted 18 July 2019
Available online 19 July 2019

Keywords:
Comprehensive two dimensional liquid chromatography
HILIC × RP
Mass spectrometry
Microalgae
Peptides

ABSTRACT

In this study, a comprehensive hydrophilic interaction chromatography × reversed phase coupled to high resolution mass spectrometry was developed for the peptide profile of microalgae formulations subjected to gastro-intestinal digestion. A BEH Amide column was employed in the first dimension, while a BIOshell ES-C18 Peptide in the second. As modulation interface, two trapping columns, in house packed with 1.9 μm fully porous monodisperse C18 particles characterized by high retention and efficiency, were tested and compared with SecurityGuard C18 cartridges, together with a dilution flow, to reduce first dimension mobile phase strength. The platform was coupled to both diode array detector and Orbitrap mass spectrometry. The developed setup provided high peak capacity (n_c: 957) in only 60 min and a good orthogonality (A_0: 0.70). The employment of the custom made C18 traps resulted in improved sensitivity (signal enhancement = 4) and a higher number of peptides detected (+58) especially of short lenght (≤ 6 aminoacids), with respect to the setup based on the security guard C18 traps. 184 phycocyanin-derived peptides were detected in Klamath and Spirulina gastro-intestinal digests, whose sequence and protein origin has been elucidated in detail by mass spectrometry. The results show the potential of the developed HILIC × RP-MS platform for in depth peptide mapping of microalgae and its possible application to highlight the products of gastro-intestinal digestion of other microalgae species.

1. Introduction

Peptidomics, a term coined by Schulz-Knappe in the 2001 [1], rely on the characterization of peptides in a biological sample. The search for bioactive peptides, especially deriving from natural or food origin, is of particular interest in drug discovery and for the pharmaceutical and nutraceutical industry. In this regard, microalgae derived peptides are particularly interesting. Microalgae are a wide group of unicellular organisms, defined as the "food of the future" since they contain numerous nutritive and healthy compounds, and especially, high percentages of proteins per dry weight [2], for these reasons, microalgae are widely used in nutraceutical formulations and functional foods. Bioactive peptides are usually encrypted in the sequence of parent proteins, they are released and become active after hydrolysis processes, such as during gastro-intestinal digestion following the oral administration of these products [3]. However, the complexity of the sample after this multi-step proteolytic process increases considerably, resulting into an enormous number of short medium length peptides with wide dynamic range. While numerous papers report the bioactivity of peptides deriving from enzymatic digestion of microalgae, there are no report concerning the complete peptide mapping of the digests, and usually only offline LC-fractionation and MALDI-MS is performed, resulting in partial peptide mapping of fractions [4]. The complexity of gastro-intestinal digests makes peptide mapping challenging. One-dimensional Liquid Chromatography coupled to Mass Spectrometry (1D-LC-MS) usually is not capable to fully resolve these samples [5] leading to unsatisfactory sequence cover-

* Corresponding author at: Department of Pharmacy, University of Salerno, Via Giovanni Paolo II 132, I-84084 Fisciano, SA, Italy.
E-mail address: pcampiglia@unisa.it (P. Campiglia).
[1] These authors equally contributed as first author.

https://doi.org/10.1016/j.jpba.2019.112783
0731-7085/

age and loss of information for low-abundant peptides that remain "hidden" behind highly abundant compounds. In order to simplify the complexity of the sample prior MS detection, high resolution separation techniques are mandatory. Comprehensive two dimensional Liquid Chromatography (LC × LC) is very useful when dealing such complex samples, and it is capable to provide higher peak capacity values with respect to 1D-LC [5]. LC × LC has been applied to peptide mapping with different stationary phase combinations such as Ion Exchange × Reversed Phase (IEX × RP) [6], Size exclusion × Reversed Phase (SEC × RP) [7], Reversed Phase × Reversed Phase (RP × RP) with different pH values [8,9] and Reversed Phase × Hydrophilic Interaction Chromatography (RP × HILIC) [10]. In the last years, driven by the biopharma sector, LC × LC has been also successfully applied to the characterization and clonal selection of monoclonal antibodies (mAbs) with both RP × RP and HILIC × RP modes [11]. The latter combination has been reported to provide a high degree of orthogonality in LC × LC [12,13], but it is hindered from solvent-strength difference between the dimensions, which causes poor peak focusing, and sample breakthrough. Different solutions have been proposed to reduce the solvent strength prior the injection in the second dimension (^{2}D) in HILIC × RP. One of the first is based on the employment of microbore (1.0 mm I.D) columns in the first dimension (^{1}D) in order to reduce the injection volume in the ^{2}D [14]. An alternative relies on the employment of trapping columns instead of sample loops, that together with the employment of a dilution flow, to reduce eluotropic strength of ^{1}D mobile phase, trap and elute the ^{1}D fractions. This last approach has been employed in online HILIC × RP peptide mapping of neuropeptides [15] showing potential respect to SCX × RP. Despite this, the online HILIC × RP coupling is still challenging, and optimization is required to ensure adequate peak focusing and sensitivity. Given the high complexity of gastro-intestinal peptide digests, in this work we present HILIC × RP-MS system with a trapping column modulation applied to microalgae peptidomics, characterized by high peak capacity and sensitivity, especially in the overall number of identified peptides. This is achieved through the implementation of two custom-made trapping columns packed with high loading and high surface area sub-2 μm monodisperse C18 fully porous particles. The HILIC × RP-MS method has been applied to the characterization of peptidome of *Aphanizomenon flos-aquae* (Klamath) and *Arthrospira Platensis* (Spirulina) microalgae dietary supplements subjected to *in vitro* simulated gastro-intestinal digestion. System performance was elucidated in terms of peak capacity, orthogonality and number of identified peptides, in the consequent coupling with MS detection.

2. Materials and methods

2.1. Chemicals

Ultra pure water (H_2O) was obtained by a Direct-8 Milli-Q system (Millipore, Milan, Italy), LC–MS grade acetonitrile (ACN) and additives formic acid (HCOOH), ammonium formate ($HCOONH_4$) phosphoric acid (H_3PO_4) and Trifluoroacetic acid (TFA) were all purchased by VWR (Milan, Italy). Enzymes Pepsin, Chymotrypsin, Pancreatin, bile salts, small molecules and peptide standard mix were all purchased by Sigma Aldrich (Milan, Italy). Klamath and Spirulina nutraceutical formulations (powders) were obtained by Farmalabor (Assago, Milan, Italy).

2.2. Protein isolation and simulated gastro-intestinal digestion

Protein extraction was carried out as reported by previously [2], briefly the Klamath or Spirulina powder (15 g) were extracted with 240 mL of 0.1 M sodium phosphate buffer (ratio w/v of 1:16), with 3 freeze-thaw cycles of 4 h (from −20 °C to 37 °C). After every cycle, the suspension was kept in ultrasonic bath for 30 min with 550 W power and, then, centrifuged (10 min at 4 °C, × 6400 rpm). The green-blue supernatant was removed and the pellet retreated with a fresh solution. Finally, all supernatants were pooled and lyophilized.

Simulated gastro-intestinal digestion was performed according to Pepe et al. [16]. An aliquot of sample was diluted with H_2O to a concentration of 10 mg/mL, the pH of solution was adjusted to 2 with HCl 0.1 N and pepsin (enzyme/protein ratio 1:100 w/w) was added. After 2 h under stirring at 37 °C, the pepsin was inactivated increasing the temperature to 90 °C for 10 min. The solvent was removed under reduced pressure, and 10 mL of a 10 mM $HCOONH_4$ solution were added and pH was adjusted to 7.5 with NH_4OH, subsequently chymotrypsin (bovine pancreas), pancreatin (from porcine pancreas) (enzyme/protein ratio 1:100 w/w) and bile salts were added. The reaction was stopped, after 2 h, by adjusting pH to 2 with TFA. The peptide fraction was concentrated and purified from salts and sugars by solid phase extraction (SPE). The fraction was solubilized in 0.1% (v/v) aqueous TFA (final concentration 10 mg/mL), and loaded on a Strata®-X Polymeric 100 mg/3 mL (Phenomenex® Castel Maggiore, Bologna, Italy) cartridge, previously equilibrated in 0.1% TFA; after loading, the sample was eluted with ACN:H_2O:TFA (70:30:0.1 v/v/v) and finally re-lyophilized and stored at −20 °C.

2.3. Columns

In HILIC × RP analyses an Acquity UPLC™ BEH Amide 150 mm × 2.1 mm, 1.7 μm (130 Å) (Waters, Millford, MA, USA) was used in ^{1}D. In ^{2}D two different columns were tested: a Titan™ C18 50 mm × 3.0 mm, 1.9 μm (80 Å) and a BIOshell™ Peptide ES C18 50 mm × 3.0 mm, 2.7 μm (160 Å) from Supelco (Bellefonte, PA, USA). For comparison purpose a Kinetex® HILIC 150 mm × 2.1 mm, 2.6 μm (100 Å), a Luna HILIC 150 mm × 2.0 mm, 3.0 μm (200 Å) (Phenomenex®) and a BIOshell™ Peptide ES C18 150 mm × 2.1 mm, 2.0 μm (160 Å) (Supelco) were also tested. In the modulation interface, the performance of two types different trapping columns were evaluated namely: SecurityGuard™ Ultra C18 2.0 mm × 3.0 mm, sub-2 μm (Phenomenex®) and two custom-made trapping columns 10 mm × 3.0 mm which were in house packed with Titan™ C18 1.9 μm (80 Å) monodisperse fully porous silica particles, kindly donated by Supelco to Professor Francesco Gasparrini.

2.4. Instrumentation

For the evaluation of kinetic and thermodynamic performances of the trapping columns an Acquity UPLC® (Waters) was employed, consisting of a binary solvent manager, a column heater (from 4 to 65 °C) and a Waters 2996 PDA detector with a 500 nL flow cell. To reduce the extra-column volume nano viper capillaries of 250 mm × 0.075 mm L. × I.D (internal volume: 1.10 μL) were used (Thermo Fisher Scientific, Milan, Italy). The total extra-column volume was determined injecting uracile by using a zero dead volume union and was estimated in 4.11 μL. The extra column peak variance, measured from the injector needle port to the detector cell, was 1.2 μL^2 (calculated through peak moments) at a flow rate of 1 mL/min.

1D-LC and HILIC × RP analyses were performed on a Shimadzu Nexera (Shimadzu, Milan, Italy), consisting of a CBM-20A controller, four LC-30AD dual-plunger parallel-flow pumps, a DGU-20 A5 degasser, an SPD-M20A PDA detector with a 2.5 μL detector flow cell, a CTO-20AC column oven, a SIL-30AC autosampler, an external oven (ThermaSphere™ TS-130 HPLC Column) was used

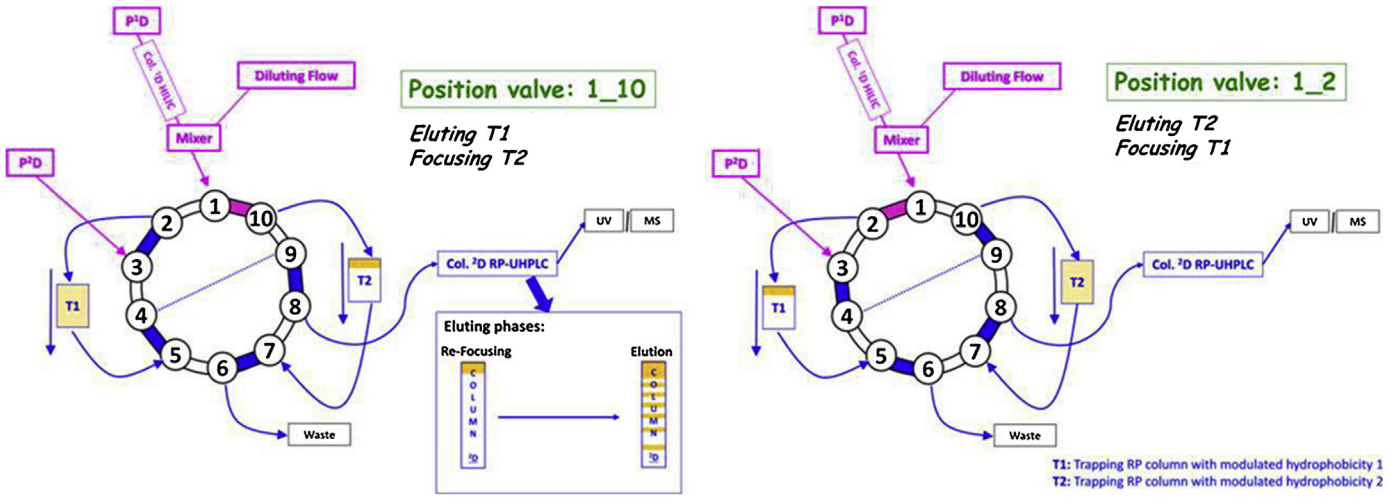

Fig. 1. Configuration of the HILIC × RP system.

for the ^{1}D column. An additional pump (external command) LC-20AT was used to deliver the post ^{1}D dilution flow (isocratic mode) by means of a stainless steel Tee union, 1/16 in. 0.15 mm bore (Vici-Valco® 167 Houston, TX 77255, USA) installed prior the valve and connected with two 0.127 mm I.D tubing. The two dimensions were connected by an ultra high pressure 10 port-two position switching valve with micro-electric actuator (model FCV-12 AH, 1.034 bar, Shimadzu, Kyoto, Japan), placed inside the column oven and equipped with two trapping columns to alternatively trap and elute fractions from ^{1}D to ^{2}D. The traps were connected to the valve by Viper capillaries of 10 cm × 0.130 mm I.D (Thermo Fisher Scientific, Milan, Italy). The valve configuration is reported in Fig. 1. A 35 cm × 0.130 mm I.D. viper capillary was used to connect the autosampler to ^{1}D column (4.6 μL), while a 10 cm × 0.130 mm I.D viper capillary was used to connect the 10 port switching valve with ^{2}D column (1.32 μL). All other connections were 0.130 mm I.D. and kept of the shortest length possible. A total extra-column volume of 28.6 μL was determined injecting uracile by using a zero dead volume union in place of the column. Both dimensions and the valve switching were controlled by the LCMS solution® software (Version 5.54, Shimadzu). The instrument was coupled online with a LTQ-Orbitrap XL (Thermo Scientific, Bremen) equipped with an electrospray source operated in positive mode. The LC × LC data were visualized into two and three dimensions using Chromsquare® ver. 1.5.01 software (Chromaleont, Messina). LC × LC-MS/MS data were aligned by MZmine2.

2.5. Chromatographic conditions: 1D-LC and HILIC × RP

1D-LC HILIC analysis were carried out with the following parameters: the mobile phases (A) and (B) consisted of 5 mM, 50 mM $HCOONH_4$ or 0.1% TFA in H_2O (v/v) (pH 6.02, pH 4.5 adjusted with HCOOH, and pH 2) and ACN respectively. Different flow rate and gradients were tested (see supporting material Fig. S1 A–C). Column oven was set at 40 °C. The PDA detector parameters were: sampling rate 40 Hz, time constant 0.1 s, wavelength 220–214 nm. 2 μL were injected.

HILIC ^{1}D mobile phase was (A): 5 mM $HCOONH_4$ in H_2O (pH 6.02), (B): ACN. ^{1}D gradient: 0–15 min, 95–80% B, 15–60 min, 80–72% B, 60–62 min, 72–60% B, returning to initial conditions in 0.1 min. Flow rate was set at 100 μL/min, column oven was set at 40 °C. 4 μL were injected (70/30 ACN/0.1% TFA in H_2O).

RP ^{2}D mobile phase was (A) 0.1% H_3PO_4 (PDA detection) or HCOOH (MS detection) in H_2O v/v, (B) ACN. In ^{2}D the gradient was operated in multi-segment shifting mode (see supporting material for detailed description). Flow rate was 2.2 mL/min. Column oven was set at 50 °C. PDA detection parameters were: sampling rate: 100 Hz, time constant 0.025 s, wavelength 220–214 nm. The modulation time was 45 s.

2.6. Mass spectrometry peptide identification

The flow from the ^{2}D was split by a Tee union prior the ESI source (approximately 400 μL/min to MS, measured with a 1 mL syringe). Detection was performed in ESI^{+} as follows: spray voltage was set at +4.5 kV, sheath gas arbitrary units 40, auxiliary gas arbitrary units 12, and capillary temperature 250 °C. MS/MS spectra were collected in data-dependent mode, over the *m/z* range of 250–2000, at 30,000 resolution. All MS/MS spectra were collected using a normalized collision energy of 35% and an isolation window of 2 *m/z*, minimum signal threshold 100, and monoisotopic precursor enabled. Ion trap and Orbitrap maximum ion injection times were set to 50 and 100 ms, respectively. Automatic gain control was used to prevent over-filling of the ion traps and was set to 2×10^{5} for full FTMS scan and 3×10^{4} ions in MS/MS mode for the linear ion trap. Dynamic exclusion was enabled with a repeat count of 1 and a repeat duration of 30 s, list size 50, with exclusion duration of 30 s. Preview mode for FTMS master scan was enabled. Thermo RAW datafiles were converted in mzXML format by ProteoWizard open source software and elaborated with a free trial of PEAKS 8.5 (Bioinformatic Solution, Waterloo, Canada) by using the DB search tool (database: *Aphanizomenon flos-aquae* and *Arthrospira Platensis*, release UniProt 2017) and *De novo* sequencing tool, mass accuracy tolerance was set at 15 ppm for MS and 0.5 Da for MS/MS, oxidation of methionine was selected as variable modification.

3. Results and discussion

Peptides deriving from gastro-intestinal (G.I) digestion processes are usually characterized by short-medium lenght amino acid sequences. As an alternative to RP, HILIC is rapidly becoming popular for the analysis of peptides. As stated before, the HILIC × RP coupling is highly orthogonal but difficult to realize due to solvent-mismatch. The benefits of multidimensional liquid chromatography have been highlighted very recently for peptide isolation and fractionation of microalgae by Montone et al. [17], but not for peptide mapping of crude g.i digest of microalgae so far.

3.1. Method development for ^{1}D (HILIC) and ^{2}D (RP) separations

3.1.1. ^{1}D: HILIC

Three different HILIC stationary phases were investigated for the separation of the microalgae G.I digests: a crosslinked diol, bare silica and amide. All columns possessed narrow-bore geometry (150 mm × 2.1 or 2.0 mm I.D) but different particle size and chemistry. Two different aqueous mobile phase were tested, with ammonium formate buffer (5 or 50 mM) or 0.1% trifluoroacetic acid, while organic phase remained acetonitrile. The effect of buffer, flow rate, gradient, injection volume and column temperature were tested. As can be appreciated by Fig. S1 (A–C), the BEH amide provided good retention as well as peak shape. A higher resolution and a different selectivity, with respect to both crosslinked diol and bare silica columns, was observed. Those results are similar with previous comparison studies on different HILIC stationary phases [18]. The best results were obtained with 5 mM $HCOONH_4$ buffer, and this was finally selected as (A) mobile phase. Furthermore, the HILIC separation was compared to a RP separation on a C18 superficially porous particle (SPP) column. Due to the chemical properties of the amino acids contained in the peptides resulting from the G.I digestion, it can be appreciated that most of the peptides eluted with very low percentage of acetonitrile in RP conditions (<15% ACN), and some were not well retained. Contrariwise, HILIC separation showed a good retention for most of the peptides (Fig. S2 A–B). In LC × LC usually ^{1}D separation is carried out with a shallow gradient at low flow rates, in order to facilitate the sampling of peaks and transfer low volumes [19]. Based on these considerations we modified both the gradient and flow rate, the final method comprised a shallow gradient from 95%B to 72%B in 60 min with a flow rate of 0.1 mL/min (Fig. S3).

3.1.2. ^{2}D: RP

In online LC × LC the sampling time is an essential parameter, since the two dimensions are connected, ^{2}D analysis time must extremely fast, to avoid the "undersampling" effect [20]. Usually, short (30–50 mm) and high efficiency columns packed with sub-3 or sub-2 μm FPP or SPP are employed, to provide an adequate sampling of the ^{1}D peaks together with high efficiency. In this work we compared two short (50 mm) C18 columns packed with 2.7 SPP and 1.9 μm monodisperse FPP, the last characterized in detail by Catani et al. [21]. The ^{2}D the separation was tuned by injecting a mixture of five peptides ranging from the dipeptide Gly-Tyr to the octapeptide Angiotensin II. For mobile phase A (water) as acidic modifier we selected 0.1% phosphoric acid for UV analyses, while 0.1% formic acid was employed only for MS detection, since it possess a larger extinction coefficient at 214 and 220 nm, which causes UV baseline shift in fast repetitive gradients, mobile phase B was acetonitrile. Flow rate, column temperature and modulation time were investigated. A flow rate of 2.2 mL/min together with column temperature of 50 °C and a total analysis time of 45 s, resulted as the best compromise in terms of resolution, re-equilibration time, and system backpressure (Fig. S4 A–B). As also reported in a previous LC × LC approach [22], the monodisperse FPP ^{2}D columns show a higher retention compared to SPP columns, which correlate with its higher surface area, and can be noticed from the different retention of the five standard peptides. In this case both columns provided similar performance, and were both tested as ^{2}D in the final method (see afterwards).

3.2. HILIC × RP coupling: trapping column evaluation

Trapping columns have been used in nanoscale SCX × RP and HILIC × RP in proteomics [23,24]. Critical parameters for peptide mapping are the retention, the chemistry and geometry of the trapping columns, in order to create I) efficient peak focusing II) trap all the peptides in the sample and III) avoid band broadening due to the dead volume between the trap and the ^{2}D column. In the present HILIC × RP approach, we compared two different setup with two type of C18 trapping columns (detailed kinetic and thermodynamic parameters are reported in Table S1). As can be appreciated in Fig. 2, the retention factors of the custom-made traps are nine times higher ($\Delta k'_{Trapping\_Titan\_C18}/\Delta k'_{SecurityGuardUltra\_C18}$ = 9.14) with respect to the C18 SecurityGuard™ trapping columns, in correlation with the very high surface area of the Titan C18 particles (410 m^2/g). This aspect is a key parameter that leads to a I) a very efficient peak focusing of peptides and furthermore II) a sensible signal enhancement. In fact, the employment of custom made FPP traps results in higher sensitivity, a crucial aspect in LC × LC, due to the intrinsic dilution of the process. Figs. 3 and 4 show respectively the 2D and 3D maps relative to the separation of Klamath G.I digest. As can be appreciated, a higher number of peaks were observed with custom made FPP traps. An average signal enhancement (SE) by a factor of 4 was calculated (Table S2), monitoring specific peptides covering the entire elution window. Given the large dynamic range in peptide digests, the implement of trapping columns with strong retentive properties and packed with particles producing small plate heights, that lead to small trap volumes, minimization of band broadening and signal enhancement [25], is highly desirable in peptidomics to detect low-abundant peptides. Slightly sharper peaks were obtained in back-flush mode, but a sensible increase of backpressure was noticed in back-flush mode, thus, to preserve system lifetime, we selected the forward-flush mode. In order to reduce the strength of acetonitrile rich ^{1}D mobile phase a dilution flow was applied. The mobile phase was water with 0.1% formic (MS detection) or phosphoric acid (UV detection) respectively. 1:2, 1:5 and 1:10 split ratio were tested, with a ^{1}D flow rate of 100 μL/min, the optimal dilution ratio prior the trapping was 1:10 (data not shown).

Table 1
Performance of HILIC × RP approach, peak capacities are corrected taking into account undersampling and orthogonalit.

Parameters		
^{1}D column geometry	Acquity UPLC™ BEH Amide 150 mm × 2.1 mm, 1.7 μm (130 Å)	
^{1}D flow rate	100 μL/min	
^{1}D column temperature	40 °C	
^{2}D column geometry	Titan™ C18 50 mm × 3.0 mm, 1.9 μm (80 Å) FPP	BIOshell™ Pepetide ES C18 50 mm × 3.0 mm, 2.7 μm (160 Å) SPP
^{2}D Flow rate	2.2 mL/min	
^{2}D column temperature	50 °C	
^{2}D gradient	Multi-segment shifting mode	
Analysis time	60 min	
Modulation time	45s	
Post ^{1}D Dilution flow	1mL/min	
Ortogonality A_0	0.61	0.70
Theoretical $2D_{nc}$	1792	1951
Practical $2D_{nc}$	766	957

3.3. Evaluation of the HILIC × RP system performance

In order to estimate the performance of the developed HILIC × RP platform, the peak capacity were calculated taking into account both undersampling and orthogonality, all the values for the different set-up are reported in Table 1. The ^{1}D peak capacity was calculated with Eq. (1)

$$1nc = \frac{\left(t_{r,l-}\, t_{r,f}\right)}{{}^1w_{avg}} \quad (1)$$

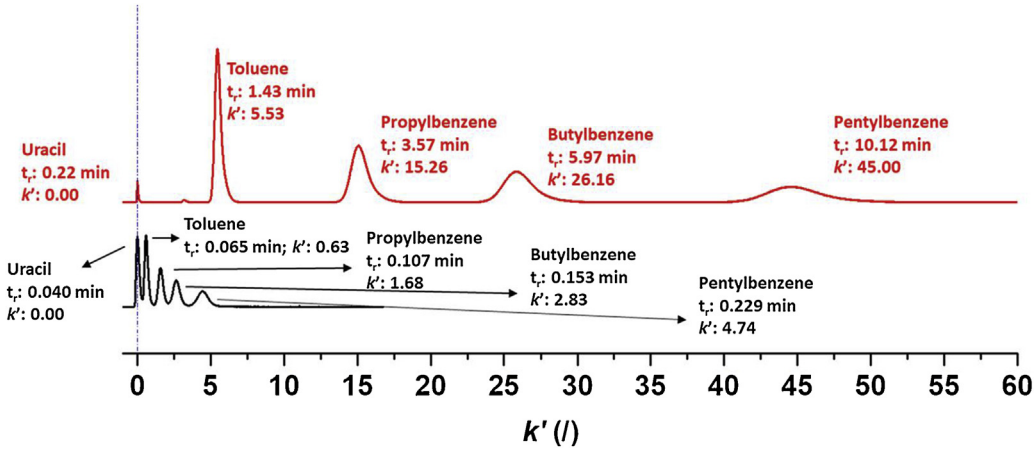

Fig. 2. Retention factor (k) comparison between the two C18 trapping columns tested. Red line: in house packed Titan™ C18 10 mm × 3.0 mm, 1.9 μm, mobile phase H_2O/ACN 50:50, column oven: 35°, flow rate 0.7 mL/min. Black line SecurityGuard™ Ultra C18 2.0 × 3.0 mm, sub-2 μm, mobile phase H_2O/ACN 50:50, column oven: 35°, flow rate 0.5 mL/min (For interpretation of the references to colour in this figure legend, the reader is referred to the web version of this article).

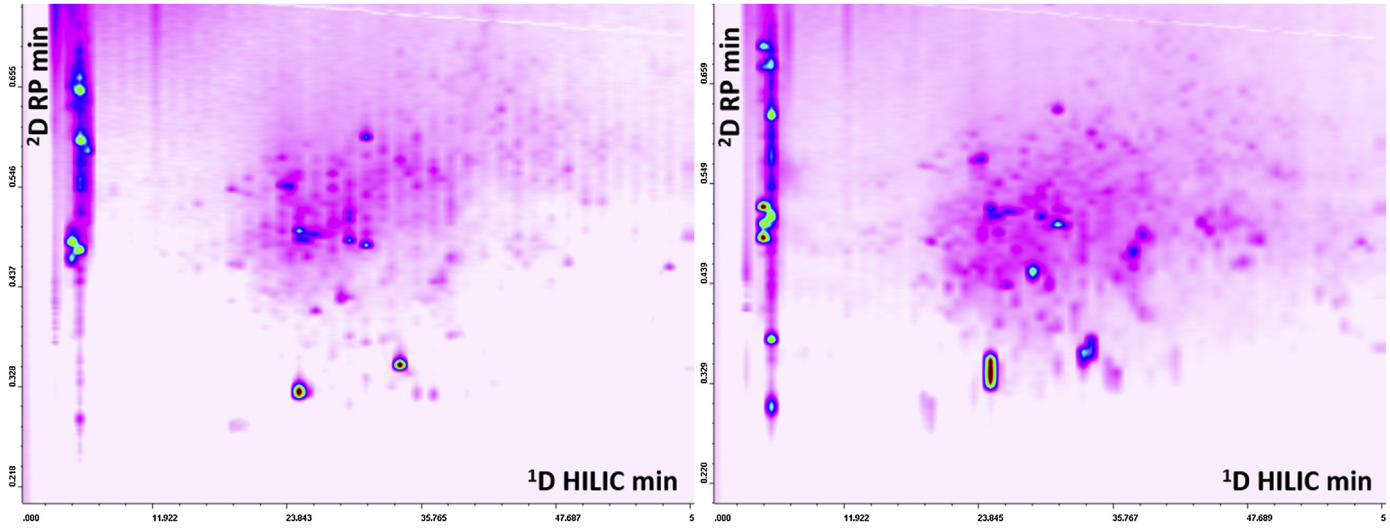

Fig. 3. HILIC × RP-UV (220 nm) plot with the different trapping columns. Sample: Klamath microalgae G.I digest, ^{1}D UPLC® BEH Amide 150 mm × 2.1 mm, 1.7 μm, ^{2}D: BIOshell™ ES C18 50 mm × 3.0 mm, 2.7 μm, Trapping columns: SecurityGuard™ Ultra C18 (left), custom-made Titan™ C18 traps (right).

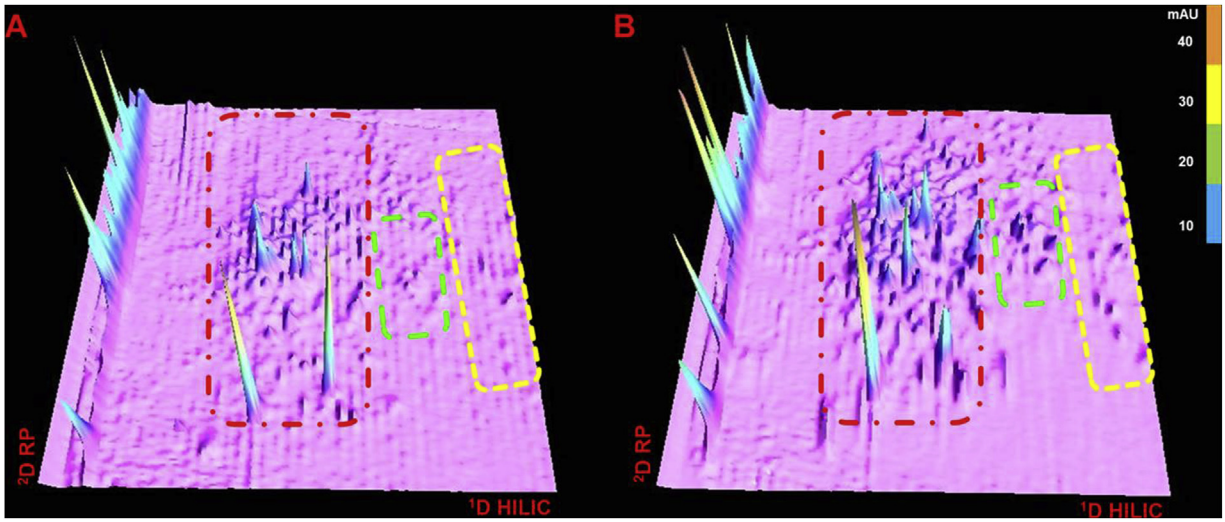

Fig. 4. a, b: 3D maps showing the signal enhancement obtained with custom made Titan™ C18 (B, right) compared to SecurityGuard™ Ultra C18 (A, left) trapping columns. Sample: Klamath microalgae G.I digest, ^{1}D UPLC® BEH Amide 150 mm × 2.1 mm, 1.7 μm, ^{2}D: BIOShell™ C18 50 mm × 3.0 mm, 2.7 μm.

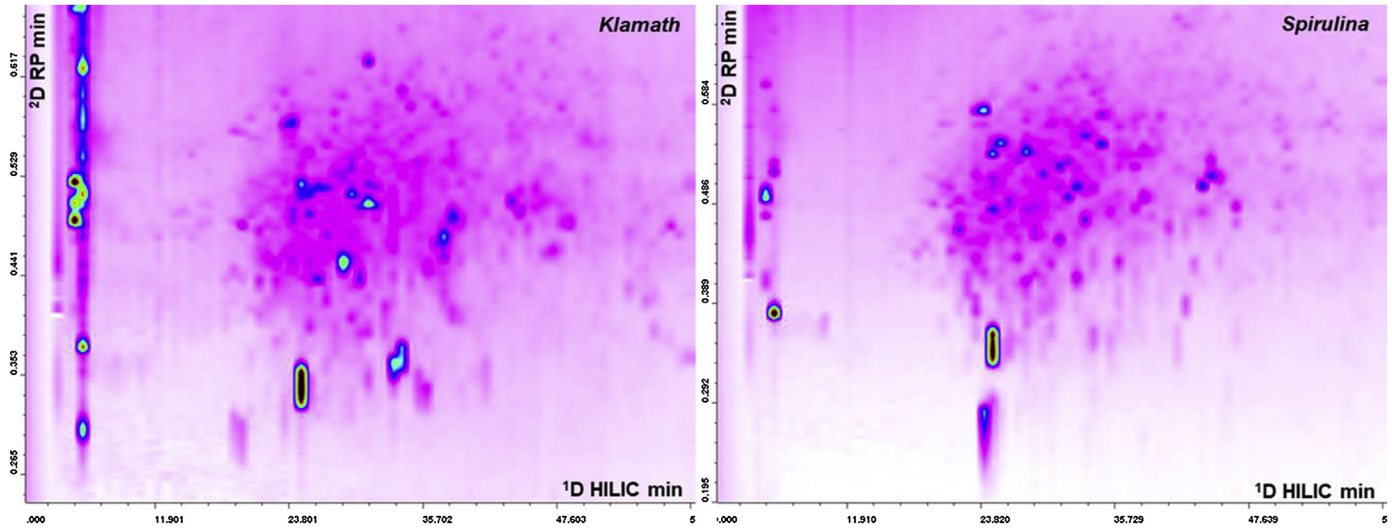

Fig. 5. 2D HILIC × RP UV (220 nm) maps of Klamath (left) and Spirulina (right) G.I digests. ^{1}D UPLC® BEH Amide 150 mm × 2.1 mm, 1.7 μm, ^{2}D: BIOShell™ C18 50 mm × 3.0 mm, 2.7 μm.

where t_r1 and t_rf are the retention times of the last and first peaks eluted in the 2D map, and $^{1}w_{avg}$ is the average 4σ peak width (^{1}D) of five selected peaks in the 2D space, covering the entire separation window, the value of 57 was obtained. The ^{2}D peak capacity was calculated according to Eq. (2):

$$2nc = \frac{^{2}t_g}{^{2}w_{avg}} \quad (2)$$

In which $^{2}t_g$ is the ^{2}D gradient time, without the re-equilibration time and $^{2}w_{avg}$ is the average 4σ peak width (^{2}D) relative to the same five peaks used previously. Values of 41 and 45 were obtained, using the FPP column and the SPP column respectively. The peak capacity of the HILIC × RP system can be calculated by multiplying the individual peak capacities according to Eq. (3):

$$n_c2D = n_{c1} \times n_{c2} \quad (3)$$

This value must be corrected taking into account the undersampling effect [26]. For the estimation of the undersampling Eq. (3) can be corrected with Eq. (4):

$$n'c,\ 2D = \frac{\left(^{1}n_c \times {}^{2}n_c\right)}{\langle\beta\rangle} \quad (4)$$

Where β is the correction factor described in the Eq. (5):

$$\beta = \sqrt{1 + 3.35\left(\frac{^{2}t_c}{1_{\overline{\omega}}}\right)^{2}} \quad (5)$$

In which $^{2}t_C$ is second dimension cycle time, and w average ^{1}D peak width. The latter, should be finally corrected considering to the correlations between the solute retention in the two dimension. For the calculation of the orthogonality (A_0) the asterisk method [27], was used. The maximum value of A_0 = 0.70 (Z−, 0.83; Z1, 0.89; Z+, 0.81; Z2, 0.81) was obtained with the enhanced trapping modulation HILIC × RP system, confirming a good orthogonality, even though a direct comparison with similar approaches on peptides in literature is not possible due to not reported values or different orthogonality calculation methods. A maximum value of 932 was obtained, which is relevant considering an analysis time of only 60 min, while most peptide mapping approaches are carried out longer gradients. As can be observed in Table 1, the highest values of peak capacity were obtained with the SPP column in the ^{2}D. Slightly narrower peaks ($4\sigma_{avgFPP}$: 0.87 vs $4\sigma_{avgSPP}$: 0.82) were obtained on the SPP column, this could be also related to difference of pore size of the SPP column (SPP:160 Å vs FPP:80 Å) which results in similar or superior kinetics with respect to FPP, for the separation of peptides at the very high flow rate such as that employed in ^{2}D, in agreement with previous observations [28]. Method repeatability was assessed by triplicate injection monitoring peak area and retention time of five selected peaks spanning in the 2D map, CV% values of 11.09 and 0.07% were obtained respectively.

3.4. HILIC × RP-MS/MS peptide mapping of Klamath and Spirulina G.I digests: peptide origin and mass distribution

The ultimate goal in peptidomics is the identification of peptide sequences derived from proteolysis process, these information can be useful to detect peptides that surviving the G.I digestion, could be absorbed and exert their activity, and thus be designed as lead compound for peptide synthesis [29]. Fig. 5 (A) and (B) show the 2D maps relative to the separation of peptide G.I digests of Klamath and Spirulina formulations. Supporting Table S3 reports the complete list of phycocyanin derived peptides identified in this study, together with *de-novo* peptides with average local confidence (ALC) comprised between 94 and 85%. While the largest body of literature report the sequence of only few peptides (usually by MALDI-MS) that are the result of isolation processes after the enzymatic digestion [4] we here reported for the first time a detailed profile of the peptides deriving from a the multi-enzymatic gastro intestinal digestion. A large number of phycobiliproteins derived peptides were detected, but in our approach we focused mainly on phycocyanin derived peptides, since they have been ascribed of numerous healthy benefits. 184 peptides were detected in the two digests, and a higher number of peptides was detected employing the custom made FPP traps for both Klamath and Spirulina digests (Table 2), with in total 58 more peptides detected with respect to the HILIC × RP method based on the two C18 SecurityGuard™ trapping columns. This is a direct consequence of the signal enhancement obtained, and can be clearly appreciated from Fig. S5 which shows the comparison of base peak chromatograms (BPC) obtained with the two different trapping approaches, in fact with a data dependent approach a higher number of low intensity precursors able to trigger the MS/MS event were selected, which on the other hand are not detected in the other setup. Interestingly, also a higher number of small chain peptides, with less of six aminoacids, were detected with the custom

Table 2
List of phycocyainin derived peptides identified in the different microalgae digest with the trapping columns packed with 1.9 FPP Titan™ C18 particles.

HILIC × RP-MS/MS identification of peptides in Klamath G.I digest

Peptide	Mass	Length	ppm	m/z	RT	Accession
AAIAGD	516.2543	6	−3.7	517.2597	36.97	P85869|PHCB_APHFL
AAIAGDA	587.2914	7	−2.3	588.2974	37.00	P85869|PHCB_APHFL
AAIAGDAS	674.3235	8	−3.1	675.3287	36.96	P85869|PHCB_APHFL
AAIAGDASV	773.3919	9	−0.6	774.3987	34.12	P85869|PHCB_APHFL
FEEQPN	762.3184	6	−3.4	382.1652	53.52	P85869|PHCB_APHFL
KTPITE	687.3803	6	−4.3	344.696	52.01	P85868|PHCA_APHFL
KTPITEA	758.4174	7	−4.4	380.2143	51.31	P85868|PHCA_APHFL
LIDGA	487.2642	5	−2.7	488.2701	30.30	P85868|PHCA_APHFL
LSNTEL	675.3439	6	−2.3	676.3497	34.86	P85868|PHCA_APHFL
M(+15.99)KTPI	604.3254	5	−3.4	303.169	46.06	P85868|PHCA_APHFL
M(+15.99)KTPIT	705.3731	6	−3.7	353.6925	46.79	P85868|PHCA_APHFL
M(+15.99)KTPITE	834.4157	7	−2.1	835.4212	52.8	P85868|PHCA_APHFL
M(+15.99)KTPITEA	905.4528	8	−4.1	453.7318	52.09	P85868|PHCA_APHFL
MKTPI	588.3305	5	−1.9	295.172	36.36	P85868|PHCA_APHFL
MKTPIT	689.3782	6	−2.4	345.6955	36.35	P85868|PHCA_APHFL
MKTPITE	818.4208	7	−2.8	410.2165	42.39	P85868|PHCA_APHFL
QALGTPGAS	800.4028	9	−1.9	401.2079	37.05	P85869|PHCB_APHFL
SKFPY	640.322	5	−1.6	641.3282	38.64	P85868|PHCA_APHFL
SNTEL	562.2598	5	−3	563.2654	42.29	P85868|PHCA_APHFL
TTSTPGNQ	804.3614	8	−4.9	805.3647	54.02	P85868|PHCA_APHFL
VAVGVGK	628.3908	7	−3.2	315.2017	46.05	P85869|PHCB_APHFL
VTGTIDQ	732.3654	7	−1.3	733.3717	37.03	P85869|PHCB_APHFL
YSKFPY	803.3854	6	−2.7	402.6989	34.93	P85868|PHCA_APHFL

HILIC × RP-MS/MS identification of peptides in Spirulina G.I digest

Peptide	Mass	Length	ppm	m/z	RT	Accession
ADSLISGA	732.3654	8	−1.2	733.3718	35.97	P72509|PHCA_ARTPT
ADSLISGAA	803.4025	9	−2.6	804.4077	36.72	P72509|PHCA_ARTPT
AGDPSIL	671.349	7	−4.2	672.3535	33.01	P72505|APCB_ARTPT
AGLEAA	530.27	6	−4.6	531.2748	33.58	P72509|PHCA_ARTPT
AIVNDPA	698.3599	7	−0.9	699.3665	41.17	P72508|PHCB_ARTPT
ALGTPGSS	688.3392	8	−4.7	689.3432	36.57	P72508|PHCB_ARTPT
ANHGL	510.255	5	−3.3	256.1339	43.94	P72509|PHCA_ARTPT
ANHGLSGDA	840.3726	9	−4.4	421.1917	52.99	P72509|PHCA_ARTPT
ANHGLSGDAA	911.4097	10	−5.5	456.7096	53.77	P72509|PHCA_ARTPT
ASEIA	489.2435	5	−5.8	490.2479	38.76	P72508|PHCB_ARTPT
ASEIAS	576.2755	6	−4	577.2805	44.75	P72508|PHCB_ARTPT
DM(+15.99)EIIL	748.3677	6	−2.8	749.3729	33.84	P72508|PHCB_ARTPT
DMEII	619.2887	5	−1.6	620.295	27.01	P72508|PHCB_ARTPT
DMEIIL	732.3727	6	−0.8	733.3795	25.55	P72508|PHCB_ARTPT
DYAIN	594.2649	5	−2.3	595.2708	35.88	P72509|PHCA_ARTPT
FAEQPQ	718.3286	6	−2.3	719.3342	39.56	P72508|PHCB_ARTPT
FATGEL	636.3119	6	−3.5	637.317	28.44	P72505|APCB_ARTPT
GIVAGDVT	730.3861	8	−1.4	731.3924	27.62	P72504|PHAA_ARTPT
GIVAGDVTPI	940.5229	10	−3.8	941.5266	23.96	P72504|PHAA_ARTPT
GLVGADAGK	786.4235	9	−3.1	394.2178	50.11	P72505|APCB_ARTPT
IAGGTGPM	702.337	8	−0.4	703.3441	29.1	P72509|PHCA_ARTPT
IAGGTGPM(+15.99)DE	962.4015	10	1.8	963.4105	50.82	P72509|PHCA_ARTPT
IAGGTGPMD	817.364	9	−1.7	818.3699	30.59	P72509|PHCA_ARTPT
IAGGTGPMDE	946.4066	10	0.6	947.414	37.38	P72509|PHCA_ARTPT
IAGID	487.2642	5	−2.5	488.2702	26.1	P72509|PHCA_ARTPT
IAGIDE	616.3068	6	−5.6	617.3106	28.37	P72509|PHCA_ARTPT
IGAMS	477.2257	5	−3.4	478.2314	26.79	P72504|PHAA_ARTPT
ITSNA	504.2544	5	−5	505.2591	37.07	P72508|PHCB_ARTPT
IVKVEL	699.4531	6	−2.2	350.733	36.02	P72508|PHCB_ARTPT
KSLGTPI	714.4276	7	−2.7	358.2201	39.69	P72504|PHAA_ARTPT
KSLGTPIE	843.4702	8	−3.8	422.7408	44.96	P72504|PHAA_ARTPT
KSLGTPIEA	914.5073	9	−2	458.26	44.22	P72504|PHAA_ARTPT
LALGTPGSS	801.4232	9	−1	802.4297	31.43	P72508|PHCB_ARTPT
LALGTPGSSV	900.4916	10	−0.1	901.4988	29.21	P72508|PHCB_ARTPT
LALGTPGSSVA	971.5287	11	−4	972.5322	29.97	P72508|PHCB_ARTPT
LDAVN	530.27	5	−3.9	531.2752	35.8	P72508|PHCB_ARTPT
LIAGI	485.3213	5	−3.9	486.3267	20.93	P72509|PHCA_ARTPT
LIAGID	600.3483	6	−2.5	601.3541	23.16	P72509|PHCA_ARTPT
LIAGIDEI	842.4749	8	−2.6	843.48	23.99	P72509|PHCA_ARTPT
LIAGIDEIN	956.5178	9	−2.5	479.265	27.73	P72509|PHCA_ARTPT
LIAGIDEINRT	1213.667	11	−2.9	607.8388	39.04	P72509|PHCA_ARTPT
LSGEDAAEA	861.3716	9	−5	862.3746	54.57	P72504|PHAA_ARTPT
LSSTE	535.249	5	−3.4	536.2544	42.32	P72509|PHCA_ARTPT
LSSTEIQ	776.3916	7	−1.6	777.3976	38.1	P72509|PHCA_ARTPT
M(+15.99)GGVAI	562.2785	6	−10.1	563.2801	30.67	P72505|APCB_ARTPT
M(+15.99)QDAIT	693.3004	6	−2.5	694.3059	41.81	P72505|APCB_ARTPT
MKTPL	588.3305	5	−2.6	589.3362	36.65	P72509|PHCA_ARTPT
NKFPY	667.3329	5	−1.8	334.6732	37.43	P72509|PHCA_ARTPT
NKFPYT	768.3806	6	−1.6	385.197	38.93	P72509|PHCA_ARTPT
NSLGVPI	698.3962	7	−5.3	699.3998	24.72	P72505|APCB_ARTPT
NSLGVPIG	755.4177	8	−2.7	756.423	26.97	P72505|APCB_ARTPT
RPDVVSPGGN	996.4988	10	−4.6	499.2544	59.09	P72504|PHAA_ARTPT
RPDVVSPGGNA	1067.536	11	−4.9	534.7726	59.86	P72504|PHAA_ARTPT
RPDVVSPGGNAYGEEM	1676.746	16	−3.2	839.3777	54.02	P72504|PHAA_ARTPT
SFVTSGE	725.3232	7	−0.8	726.3299	35.89	P72504|PHAA_ARTPT
SLGTPI	586.3326	6	−2.7	587.3383	24.66	P72504|PHAA_ARTPT
SLGTPIE	715.3752	7	−1	716.3817	29.17	P72504|PHAA_ARTPT
SLGTPIEA	786.4123	8	0.7	787.4201	30.7	P72504|PHAA_ARTPT
SPGEL	501.2435	5	−2.8	502.2493	35.12	P72504|PHAA_ARTPT
TPLTEA	630.3224	6	−2	631.3285	34.38	P72509|PHCA_ARTPT
TTQMQGPN	875.3807	8	−2.7	438.6964	47.03	P72509|PHCA_ARTPT
VAVGVGK	628.3908	7	−3.4	315.2016	47.83	P72508|PHCB_ARTPT
VVSAA	445.2536	5	−4.7	446.2588	30.45	P72508|PHCB_ARTPT
YFATGEL	799.3752	7	−1.1	800.3816	26.21	P72505|APCB_ARTPT
YSDITRPG	907.4399	8	−3.9	454.7255	44.88	P72505|APCB_ARTPT

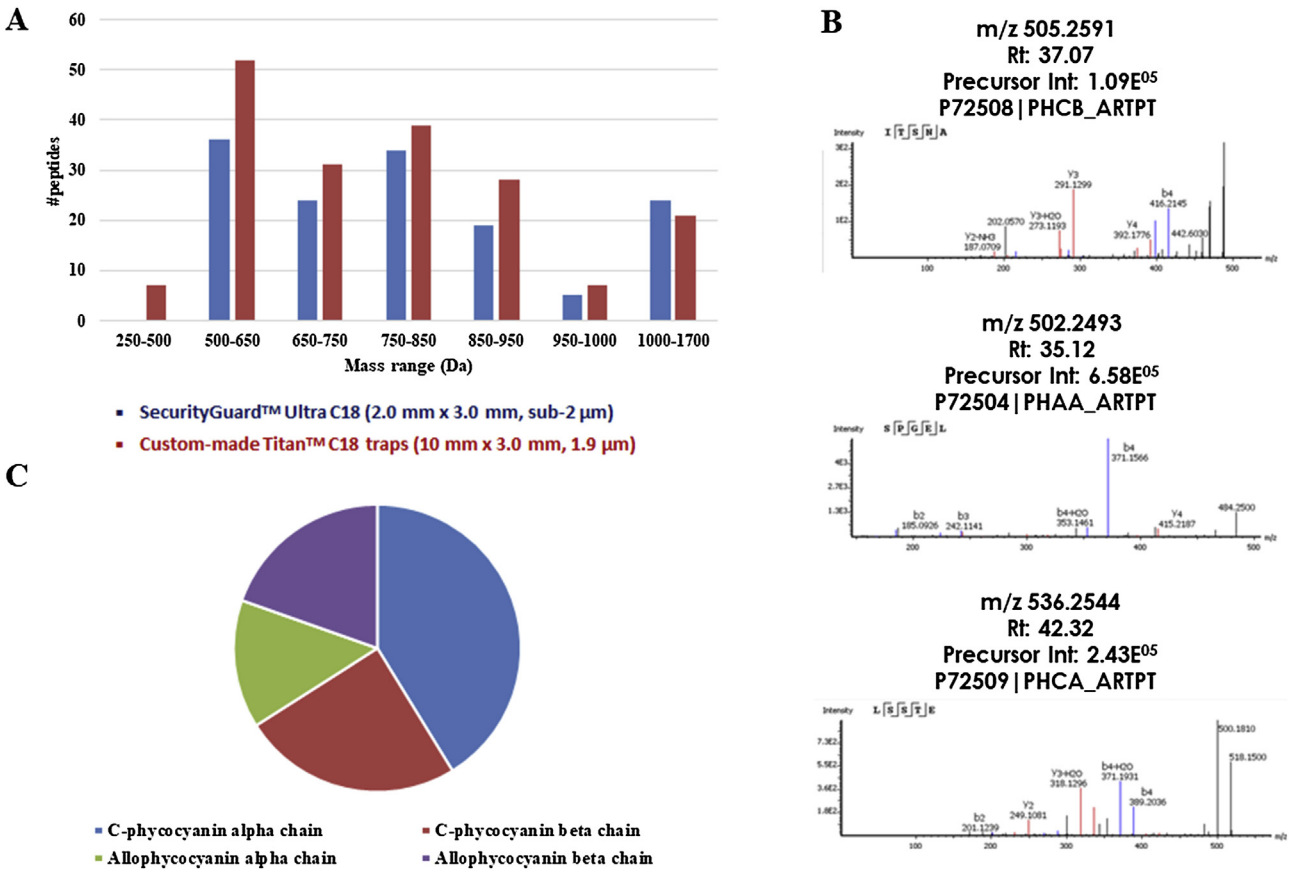

Fig. 6. a, b,c Mass distribution (a), peptide spectra (b) and origin (c) of phycocyanin derived peptides detected in Klamath and Spirulina G.I. digests.

traps (Fig. 6 A, B). This is particularly interesting in peptidomics, small peptides, composed by less than 6 aminoacids and are usually better absorbed with respect to larger peptides [16]. Peptides with less than 7 residues were the most represented in both Klamath and Spirulina digests, which is clearly correlated to the multiple cleavages that peptide sequences undergo during the multi-enzymatic process. Fig. 6 (C), show the origin of peptides, as can be observed almost half (40%) of identified peptides belong from C-phycocyanin alpha chain, while the rest from C-phycocyanin beta chain (24%) and from Allophycocyanin (alpha: 14% and beta: 19%). Allophycocyanin peptides are of particular interest, in fact, recent studies [3] reported anti-hypertensive properties of allophycocyanin derived peptides. It must be pointed out that despite a good mass accuracy (average error: -2.6 ppm) in this study we were limited from the duty cycle of the LTQ-Orbitrap-MS employed, due to the very narrow peaks of LC × LC. In this regard a higher number of peptides could be detected by employing a MS device with higher acquisition rates and fast duty cycles such as latest generation Q-Orbitrap or Q-TOF. As recently demonstrated, the employment of Ion-mobility Q-TOFs coupled to LC × LC has showed impressive results in terms of peak capacity for natural compounds [30].

4. Conclusion

Despite growing data regarding the bioactivity of microalgae peptides, there is a lack of knowledge regarding the peptides originates from gastro intestinal digestion process. The analysis of these peptide digests represents a challenge for analytical methods. LC × LC—MS employing different stationary phase combinations, such as HILIC × RP can be a valid analytical tool, but is hindered from solvent strength differences, that lead to poor peak focusing and band broadening, and furthermore, from loss of sensitivity due to sample breakthrough and excessive dilution. The present HILIC × RP approach, based on the employment a trapping columns interface provided high peak capacity values. Higher sensitivity can be obtained by employing trapping columns packed with high retentive and efficient fully porous monodisperse particles. The further hyphenation with mass spectrometry enabled the detection of a higher number of peptides, from two gastro-intestinal digests of Klamath and Spirulina microalgae formulations. The results point out the developed HILIC × RP method a valid tool for microalgae peptidomics.

Acknowledgments

This project was supported by a 2014 to 2020 PON (Programmi Operativi Nazionali) Ricerca e Innovazione grant from the Italian Ministry of Education, University and Research (MIUR), entitled PROGEMA - Processi Green per l'Estrazione di Principi Attivi e la Depurazione di Matrici di Scarto e Non (ARS01_00432) to P. Campiglia.

Appendix A. Supplementary data

Supplementary material related to this article can be found, in the online version, at doi:https://doi.org/10.1016/j.jpba.2019.112783.

References

[1] P. Schulz-Knappe, H.D. Zucht, G. Heine, M. Jürgens, R. Hess, M. Schrader, Peptidomics: the comprehensive analysis of peptides in complex biological mixtures, Comb. Chem. High Throughput Screen. 4 (2001) 207–217.

[2] E. Sommella, G.M. Conte, E. Salviati, G. Pepe, A. Bertamino, C. Ostacolo, F. Sansone, F.D. Prete, R.P. Aquino, P. Campiglia, Fast profiling of natural pigments in different Spirulina (Arthrospira platensis) dietary supplements by DI-FT-ICR and evaluation of their antioxidant potential by pre-column DPPH-UHPLC assay, Molecules 23 (2018) 1152.
[3] A. Carrizzo, G.M. Conte, E. Sommella, A. Damato, M. Ambrosio, M. Sala, M.C. Scala, R.P. Aquino, M. De Lucia, M. Madonna, F. Sansone, C. Ostacolo, M. Capunzo, S. Migliarino, S. Sciarretta, G. Frati, P. Campiglia, C. Vecchione, Novel potent decameric peptide of Spirulina platensis reduces blood pressure levels through a PI3K/AKT/eNOS-Dependent mechanism, Hypertension 73 (2019) 449–457.
[4] Z. Wang, Z.X. Zhang, Characterization and antitumor activity of protein hydrolysates from Arthrospira platensis (Spirulina platensis) using two-step hydrolysis, J. Appl. Phycol. 28 (2016) 3379–3385.
[5] P. Donato, F. Cacciola, L. Mondello, P. Dugo, Comprehensive chromatographic separations in proteomics, J. Chromatogr. A 1218 (2011) 8777–8790.
[6] T. Kajdan, H. Cortes, K. Kuppannan, S.A. Young, Development of a comprehensive multidimensional liquid chromatography system with tandem mass spectrometry detection for detailed characterization of recombinant proteins, J. Chromatogr. A 1189 (2008) 183–195.
[7] F. Bedani, W.Th. Kok, H.G. Janssen, A theoretical basis for parameter selection and instrument design in comprehensive size-exclusion chromatography × liquid chromatography, J. Chromatogr. A 1133 (2006) 126–134.
[8] P. Donato, F. Cacciola, E. Sommella, C. Fanali, L. Dugo, M. Dachà, P. Campiglia, E. Novellino, P. Dugo, L. Mondello, Online comprehensive RPLC × RPLC with mass spectrometry detection for the analysis of proteome samples, Anal. Chem. 83 (2011) 2485–2491.
[9] E. Sommella, G. Pepe, G. Ventre, F. Pagano, M. Manfra, G. Pierri, O.H. Ismail, A. Ciogli, P. Campiglia, Evaluation of two sub-2 μm stationary phases, core-shell and totally porous monodisperse, in the second dimension of on-line comprehensive two dimensional liquid chromatography, a case study: separation of milk peptides after expiration date, J. Chromatogr. A 1375 (2015) 54–61.
[10] A. D'Attoma, S. Heinisch, On-line comprehensive two dimensional separations of charged compounds using reversed-phase high performance liquid chromatography and hydrophilic interaction chromatography. Part II: application to the separation of peptides, J. Chromatogr. A 1306 (2013) 27–36.
[11] K. Sandra, M. Steenbeke, I. Vandenheede, G. Vanhoenacker, P. Sandra, The versatility of heart-cutting and comprehensive two-dimensional liquid chromatography in monoclonal antibody clone selection, J. Chromatogr. A 1523 (2017) 283–292.
[12] P. Jandera, Stationary phases for hydrophilic interaction chromatography, their characterization and implementation into multidimensional chromatography concepts, J. Sep. Sci. 31 (2008) 1421–1437.
[13] M. Gilar, P. Olivova, A.E. Daly, J.C. Gebler, Orthogonality of separation in two-dimensional liquid chromatography, Anal. Chem. 77 (2005) 6426–6434.
[14] K.M. Kalili, J. Vestner, M. Stander, A. de Villiers, Toward unraveling grape tannin composition: application of online hydrophilic interaction chromatography × reversed-phase liquid chromatography-time-of-flight mass spectrometry for grape seed analysis, Anal. Chem. 85 (2013) 9107–9115.
[15] A. Mihailova, H. Malerød, S.R. Wilson, B. Karaszewskl, R. Hauser, E. Lundanes, T. Greibrokk, Improving the resolution of neuropeptides in rat brain with on-line HILIC-RP compared to on-line SCX-RP, J. Sep. Sci. 31 (2008) 459–467.
[16] G. Pepe, E. Sommella, G. Ventre, M.C. Scala, S. Adesso, C. Ostacolo, S. Marzocco, E. Novellino, P. Campiglia, Antioxidant peptides released from gastrointestinal digestion of "Stracchino" soft cheese: characterization, in vitro intestinal protection and bioavailability, J. Func. Foods 26 (2016) 494–505.
[17] C.M. Montone, A.L. Capriotti, C. Cavaliere, G. La Barbera, S. Piovesana, R. Zenezini Chiozzi, A. Laganà, Peptidomic strategy for purification and identification of potential ACE-inhibitory and antioxidant peptides in Tetradesmus obliquus microalgae, Anal. Bioanal. Chem. 410 (2018) 3573–3586.
[18] M. Gilar, A. Jaworski, Retention behavior of peptides in hydrophilic-interaction chromatography, J. Chromatogr. A 1218 (2011) 8890–8896.
[19] P. Dugo, F. Cacciola, T. Kumm, G. Dugo, L. Mondello, Comprehensive multidimensional liquid chromatography: theory and applications, J. Chromatogr. A 1184 (2008) 353–368.
[20] R.E. Murphy, M.R. Schure, J.P. Foley, Effect of sampling rate on resolution in comprehensive two-dimensional liquid chromatography, Anal. Chem. 70 (1998) 1585–1594.
[21] M. Catani, O.H. Ismail, A. Cavazzini, A. Ciogli, C. Villani, L. Pasti, C. Bergantin, D. Cabooter, G. Desmet, F. Gasparrini, D.S. Bell, Rationale behind the optimum efficiency of columns packed with new 1.9μm fully porous particles of narrow particle size distribution, J. Chromatogr. A 1454 (2016) 78–85.
[22] E. Sommella, O.H. Ismail, F. Pagano, G. Pepe, C. Ostacolo, G. Mazzoccanti, M. Russo, E. Novellino, F. Gasparrini, P. Campiglia, Development of an improved online comprehensive hydrophilic interaction chromatography × reversed-phase ultra-high-pressure liquid chromatography platform for complex multiclass polyphenolic sample analysis, J. Sep. Sci. 40 (2017) 2188–2197.
[23] H. Liu, J.W. Finch, J.A. Luongo, G.Z. Li, J.C. Gebler, Development of an online two-dimensional nano-scale liquid chromatography/mass spectrometry method for improved chromatographic performance and hydrophobic peptide recovery, J. Chromatogr. A 1135 (2006) 43–51.
[24] S.R. Wilson, M. Jankowski, M. Pepaj, A. Mihailova, F. Boix, G.Vivo Truyols, 2D LC separation and determination of bradykinin in rat muscle tissue dialysate with on-line SPE-HILIC-SPE-RP-MS, Chromatographia 66 (2007) 469–474.
[25] J. De Vos, S. Eeltink, G. Desmet, Peak refocusing using subsequent retentive trapping and strongeluent remobilization in liquid chromatography: a theoretical optimization study, J. Chromatogr. A 1381 (2015) 74–86.
[26] M.R. Filgueira, Y. Huang, K. Witt, C. Castells, P.W. Carr, Improving peak capacity in fast on line comprehensive two-dimensional liquid chromatography with post first dimension flow splitting, Anal. Chem. 83 (2011) 9531–9539.
[27] M. Camenzuli, P.J. Schoenmakers, A new measure of orthogonality for multidimensional chromatography, Anal. Chim. Acta 838 (2014) 93–101.
[28] S.A. Schuster, B.E. Boyesa, B.M. Wagner, J.J. Kirkland, Fast high performance liquid chromatography separations for proteomic applications using Fused-Core® silica particles, J. Chromatogr. A 1228 (2012) 232–241.
[29] S. Piovesana, A.L. Capriotti, C. Cavaliere, G. La Barbera, C.M. Montone, R. Zenezini Chiozzi, A. Laganà, Recent trends and analytical challenges in plant bioactive peptide separation, identification and validation (Review), Anal. Bioanal. Chem. 410 (2018) 3425–3444.
[30] P. Venter, M. Muller, J. Vestner, M.A. Stander, A.G.J. Tredoux, H. Pasch, A. de Villiers, Comprehensive three-dimensional LC × LC × ion mobility spectrometry separation combined with high-resolution MS for the analysis of complex samples, Anal. Chem. 90 (2018) 11643–11650.